BUBBLE PROPAGATION IN FLEXIBLE CHANNELS WITH PERMEABLE WALLS

M.K. HORSBURGH
DAMTP, University of Cambridge, Silver Street, Cambridge CB3 9EW, UK
M.K.Horsburgh@damtp.cam.ac.uk

O.E. JENSEN
Division of Theoretical Mechanics, School of Mathematical Sciences,
University of Nottingham, University Park, Nottingham NG7 2RD, UK
Oliver.Jensen@nottingham.ac.uk

Abstract A theoretical model is presented analysing the effects of wall permeability on the steady motion of a semi-infinite bubble advancing into a planar, flexible-walled, fluid-filled channel. Weak permeability is shown to have a profound influence, eliminating in particular the minimal yield pressure required for steady motion in an impermeable channel.

Keywords: Airway reopening; membrane permeability; thin-film flow

1. INTRODUCTION

The lungs are formed by a large bifurcating network of airways which have compliant, liquid-lined and permeable walls. Capillary–elastic instabilities can cause peripheral airways to become occluded with lining fluid at low lung volumes (Grotberg 1994), and then to collapse along much of their length under low capillary pressures. Airway flooding and collapse can be a serious problem in diseases such as respiratory distress syndrome, cystic fibrosis, emphysema and asthma. Understanding how a closed airway can be reopened by an advancing bubble of air is therefore of fundamental importance in pulmonary mechanics, and is relevant in particular to the mechanism whereby air first enters fluid-filled lungs immediately after birth.

This issue was addressed theoretically by Gaver *et al.* (1996), who modelled an airway as a two-dimensional channel formed by membranes held under tension and supported externally by springs. The opening

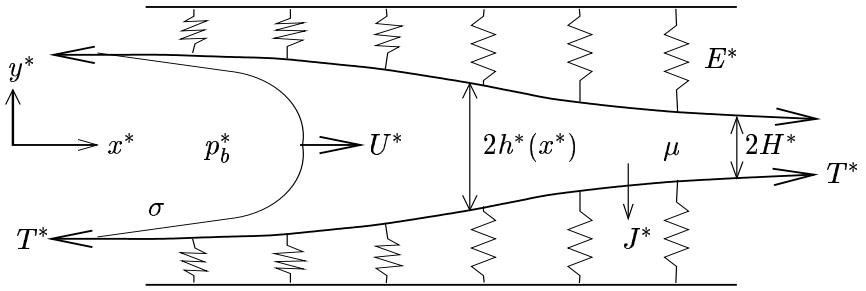

Figure 1 The permeable-walled airway opening model.

process was modelled by a bubble at fixed pressure p_b^* propagating along the initially fluid-filled channel at constant speed U^*. It was shown that, in accordance with experiment, p_b^* increases with U^* provided p_b^* is in excess of a critical value. A further steady solution branch was identified for which p_b^* diminishes with U^*, but this has since been shown to be unstable (Horsburgh 2001). Because airway walls are permeable, and because transmural fluxes are known to be an important mechanism for the clearance of fluid from the lungs after the first breath, we sought to answer the following question: what effect does airway wall permeability have on this model of airway reopening?

2. THE MODEL

Our model is illustrated in Figure 1. It consists of a two-dimensional, flexible-walled channel that is opened by a semi-infinite bubble held at pressure p_b^* propagating from left to right with speed U^*. The walls of the channel are formed by membranes held under uniform tension T^*, supported by linearly elastic springs with stiffness E^*. The separation of the membranes in stress-free conditions far ahead of the bubble is $2H^*$. The fluid occupying the channel has uniform viscosity μ and the surface tension of the advancing air-liquid interface is σ. Cartesian coordinates (x^*, y^*) are adopted with $(0, 0)$ fixed at the advancing bubble tip, with directions as shown in Figure 1. The membranes lie at $y^* = \pm h^*(x^*)$, and the flow is assumed to be symmetric about $y^* = 0$.

The novel feature of this model is the incorporation of wall permeability. The loss of fluid across the membrane at $y^* = h^*(x^*)$ is governed by Starling's law of membrane filtration, so that the transmural area flux per unit length is $J^* = K^* p^*$ (neglecting any osmotic effects), where K^* is the membrane's uniform permeability and p^* the fluid pressure at the membrane; the pressure outside the channel is taken to be zero.

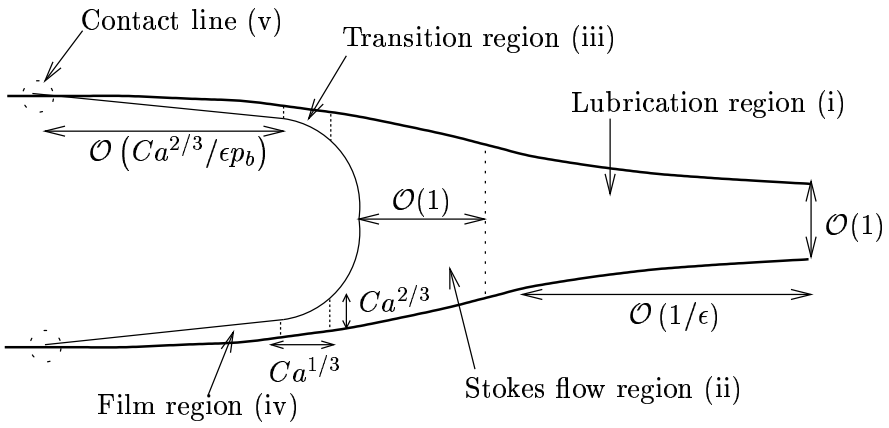

Figure 2 Asymptotic regions of the flow when $\epsilon \ll Ca \ll 1$.

Non-dimensionalisation of this problem yields five non-dimensional parameters: two wall paramters, a bubble pressure, a capillary number (a bubble speed) and a permeability parameter, defined respectively by

$$E = \frac{\epsilon E^* H^{*2}}{\mu U^*}, \quad T = \frac{\epsilon^3 T^*}{\mu U^*}, \quad p_b = \frac{K^* p_b^*}{\epsilon U^*}, \quad Ca = \frac{\mu U^*}{\sigma}, \quad \epsilon^2 = \frac{\mu K^*}{H^*}.$$

We seek p_b in terms of Ca, ϵ, E and T in the limit $\epsilon \ll Ca \ll 1$ by using matched asymptotics, assuming the motion is steady. We expect ϵ to be small since it represents the ratio of membrane pore permeability to channel permeability. Provided the bubble advances slowly, so that $Ca \ll 1$, the bubble tip is approximately a semi-circular cap which almost fills the channel. The solution domain can then be divided into the five regions illustrated in Figure 2. From right to left, these are (i) a long region governed by lubrication theory, within which almost all the fluid escapes through the walls; (ii) a short region ahead of the bubble tip where the flow is fully two-dimensional; (iii) a short transition region across which the interfacial curvature and fluid pressure vary rapidly; (iv) a thin, nearly-flat passive film deposited on the channel wall, which leaks slowly through the channel walls; and (v) a region near the receding contact line at the trailing edge of the film.

Regions (ii) and (iii) are too short for there to be significant transmural fluxes. Region (iii) is the familiar transition region of Landau & Levich (1942) and Bretherton (1961), which controls the thickness of the film deposited on the channel wall. This film is slowly pushed across the membrane by the imposed bubble pressure until it reaches region (v), where pressure gradients are generated over a lengthscale $\mathcal{O}\left(\epsilon^2/Ca\right)$ and the film thickness is $\mathcal{O}\left(\epsilon^3 p_b/Ca\right)$. We assume the air-liquid interface

ultimately meets the membrane with zero contact angle (although in the lung it is likely that disjoining pressures may prevent airway walls from becoming dry). Despite imposing a no-slip condition, the usual moving-contact-line stress singularity is relieved in this case by allowing the fluid to drain through the wall, leaving a section of wall dry which was previously wet. Similar regularisation has been noted for advancing contact lines on permeable surfaces (e.g. Davis & Hocking 1999).

The dimensionless bubble pressure has three contributions, $p_b = p_t + p_s + p_l$, where $p_t = \mathcal{O}(\epsilon/Ca)$ is the pressure drop across the transition region (iii), $p_s = \mathcal{O}(\epsilon)$ is the pressure drop across the Stokes region (ii) and $p_l = \mathcal{O}(1)$ is the pressure at the boundary between the lubrication and Stokes regions. Thus for $\epsilon \ll Ca \ll 1$, the leading order bubble pressure is given by the pressure drop across the lubrication region (i), i.e. $p_b = p_l$. We will see below that p_l is a function only of E and T, which may then be used to relate p_b^* to U^*.

3. THE LUBRICATION REGION

Here we set $x^* = (H^*/\epsilon)x$, $h^*(x^*) = H^* h(x)$ and $p^* = (\epsilon U^*/K^*)p$, so that with error $\mathcal{O}(\epsilon^2)$ the governing equations reduce to

$$p = E(h-1) - T\frac{d^2h}{dx^2}, \quad Q = -\frac{h^3}{3}\frac{dp}{dx} - h, \quad \frac{dQ}{dx} = -p. \tag{1.1}$$

Equation (1.1a) relates fluid pressure to wall displacement, (1.1b) relates the horizontal flux of fluid Q in the upper half-channel to flows driven by pressure gradients in the moving frame of the bubble tip and (1.1c) is a statement of mass conservation allowing for leakage through the channel walls. The boundary condition far ahead of the bubble tip is that the channel is in its unstressed state, so $h \to 1$ as $x \to \infty$. At the bubble tip, the wall slope must match that in the film region, so with error $\mathcal{O}(\epsilon/Ca)$,

$$h(0) = 1 + \frac{p(0)}{E} + \sqrt{\frac{T}{E}}\frac{dh}{dx}(0), \tag{1.2}$$

(a condition derived using (1.1a) with $p = p_l \equiv p(0)$, assuming $h_x \to 0$ as $x \to -\infty$). The Stokes region is too short for any significant quantity of fluid to leave through the walls, and the transition region determines that the flux flowing out of the Stokes region is $\mathcal{O}\left(Ca^{2/3}h(0)\right)$, so provided $h(0) = O(1)$ we may assume $Q(0) = 0$. Equations (1.1, 1.2) and the corresponding boundary conditions were solved either by shooting from a downstream limiting solution upstream towards the bubble tip and stopping when the flux condition at the bubble tip was satisfied (when

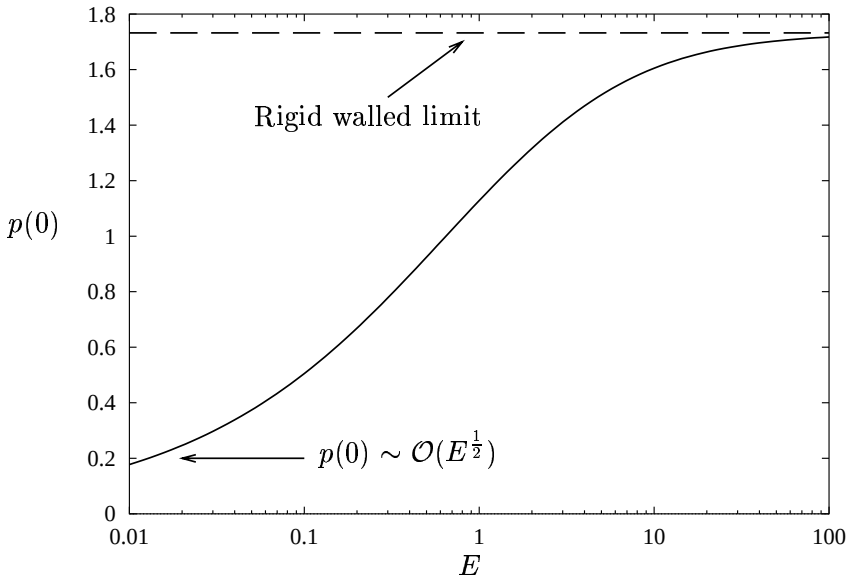

Figure 3 Bubble pressure versus the wall elasticity parameter for purely elastic walls.

$T = 0$), or by using Newton's method to solve a a finite difference approximation of the problem (when $T > 0$).

4. RESULTS

The Effect of Wall Elasticity. In order to isolate the effects of wall elasticity and tension, it is useful to consider first the case where $T = 0$, so the displacement of the wall is governed purely by its elastic support. Figure 3 shows how the bubble pressure $p(0)$ depends only weakly on E, with four orders-of-magnitude change in E causing only a single order-of-magnitude change in bubble pressure.

For $E \gg 1$, the solution approaches the rigid-walled limit $p(0) = \sqrt{3}$. When the channel is extremely compliant ($E \ll 1$), a distinctive solution results for which the bubble tip pushes a very fat, long plug of fluid ahead of it, as illustrated in Figure 4. This figure also illustrates a general property of this system. In the bubble-tip reference frame, a pair of counter-rotating vortices are formed ahead of the bubble tip. Lubrication theory is only able to resolve the right-hand side of these vortices, but fully two-dimensional calculations are able to close the streamlines in the Stokes region (Horsburgh 2001). Thus when $E \ll 1$, the bubble pushes ahead of itself a large volume of trapped fluid that never escapes through the channel walls. This 'pushing' mode is

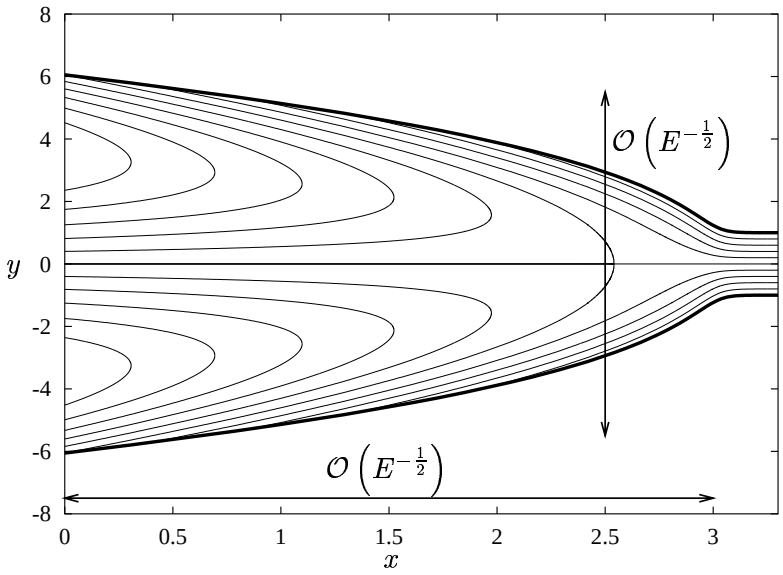

Figure 4 Streamlines in the bubble-tip reference frame (the flow enters from the right), for purely elastic walls with $E = 0.1$, $T = 0$ (the 'pushing' mode).

amenable to analysis by matched asymptotics, which shows that the vortices have length and width $\mathcal{O}\left(E^{-1/2}\right)$, and at their tip is a small region of $\mathcal{O}(E)$ length across which the wall adjusts to the downstream boundary condition. This analysis predicts that $p(0) \sim 12^{1/4}E^{1/2} - \frac{19}{14}E + \mathcal{O}\left(E^{3/2}\right)$, in excellent agreement with Figure 3. It follows that for $E \ll 1$, $p_b^* \propto U^{*1/2}$, and for $E \gg 1$, $p_b^* \propto U^*$; thus p_b^* always increases monotonically with U^* when $T = 0$.

The Effect of Wall Tension. Figure 5 shows how $p(0)$ has an even weaker dependence on T than on E when $T > 0$. However, wall tension has an enormous effect on the structure of the solution when $T \gg E$, as illustrated in Figure 6. Here, fluid is pushed across the channel walls over an $\mathcal{O}(1)$ lengthscale ahead of the bubble tip. However, the high wall tension causes the membrane to bend over a much larger, $\mathcal{O}(T/E)$ length-scale; the membrane's curvature makes the fluid pressure negative (a feature characteristic of peeling motions; see McEwan & Taylor 1966), and this draws fluid into the channel far ahead of the bubble before it is expelled again closer to $x = 0$. An asymptotic solution for $T \gg E$ shows that $p(0) \sim \sqrt{3/h(0)}$ where $4E^2h(0)(h(0)-1)^2 = 3$, so that $p(0) \propto E^{1/3}$ for $E \ll 1$, in agreement with Figure 5 (Horsburgh 2001).

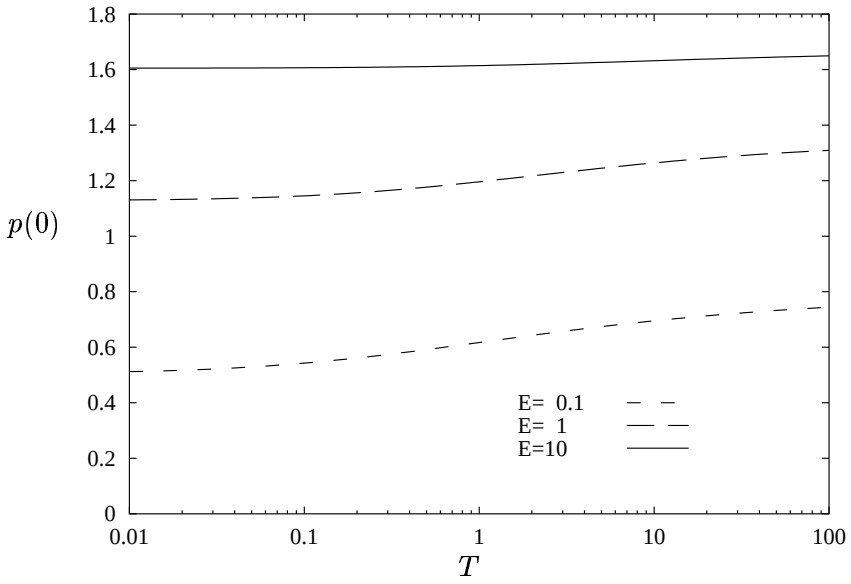

Figure 5 Bubble pressure versus the wall tension parameter T for various values of the wall elasticity parameter E.

5. CONCLUSIONS

Bubble motion in a flexible channel with *impermeable* walls exhibits two types of motion (Gaver *et al.* 1996): a pushing mode at small bubble speeds ($Ca \ll 1$) for which bubble pressure p_b^* falls with U^*; and a peeling mode at larger Ca for which p_b^* increases with U^*. Weak wall permeability dramatically changes this picture. At low speeds, with $\epsilon \ll Ca \ll 1$ (so that negligible fluid escapes past the bubble tip), p_b^* always increases with U^*. Wall properties determine whether pushing or peeling modes arise: when the channel is highly compliant ($E \ll 1$, $T = 0$), the bubble advances in a *pushing* mode with a large volume of fluid trapped ahead of bubble tip (Figure 4); high wall tension ($E \ll T$) leads to a *peeling* mode with weak inflow ahead of bubble tip (Figure 6). A large increase in wall compliance reduces the pressure required to push the bubble along the channel (Figures 3 & 5). However, for compliant channels there turns out to be an upper bound, of $O\left((\sigma^2 H^{*4} E^{*5}/\mu K)^{1/7}\right)$, on the pressure at which either type of pushing mode can exist, since for p_b^* of this magnitude the flux of fluid leaking past the bubble tip is comparable with that leaking through the channel walls (Horsburgh 2001). For pressures larger than this, a permeable channel will peel open as if it were impermeable.

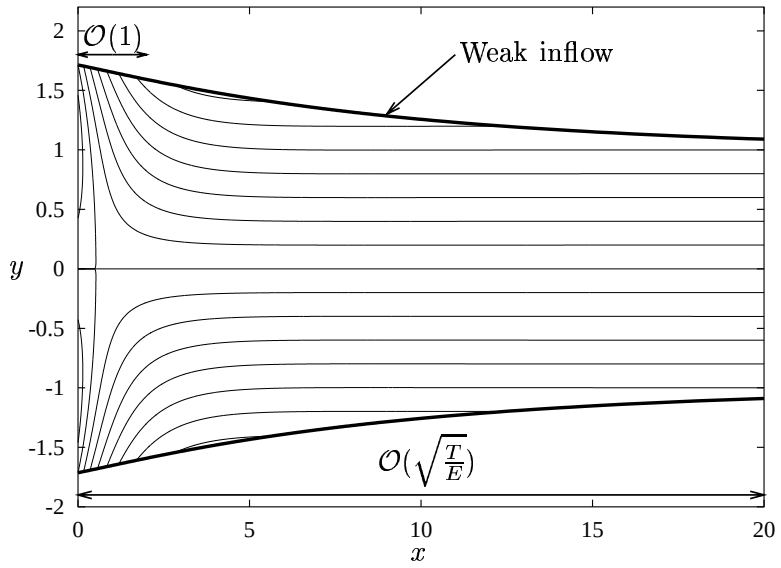

Figure 6 Streamlines in the bubble-tip reference frame for $E = 1$, $T = 100$. The flow is from right to left.

Application to lung airways. Airway wall permeability can be estimated as $K^* \approx R\alpha/\mu$ where R is the size of a pore between epithelial cells and α is the area fraction occupied by these pores. If $\alpha \sim 10^{-2}$ and $R \approx 1\text{nm}$, then $\epsilon \approx 10^{-4}$ for a 1mm airway. This suggests that the viscous pressure drop in the lubrication region is distributed over many airways, and dilution effects due to airway branching and unsteadiness due to finite network length will both be significant. These represent important future extensions of this model. However our results suggest that weakly permeable compliant airways can behave as if they were effectively impermeable under normal ventilatory pressures.

References

Bretherton, F.P. 1961 *J. Fluid Mech.* **10**, 166-188.

Davis, S.H. & Hocking, L.M. 1999 *Phys. Fluids* **11**, 1, 48–57.

Gaver, D.P., Halpern, D., Jensen, O.E. & Grotberg, J.B. 1996 *J. Fluid Mech.* **319**, 25–65.

Grotberg, J.B. 1994 *Ann. Rev. Fluid Mech.* **16**, 529–571.

Horsburgh, M.K. 2001 Ph.D. Thesis, University of Cambridge.

Landau, L. & Levich, B. 1942 *Acta Phys-chim.* URSS **17**, (1–2), 42–54.

McEwan, A.D. & Taylor, G.I. 1966 *J. Fluid Mech.* **26**, 1–15.